A WIDE BAND RING SLOT ANTENNA

INTEGRATED RECEIVER.

Andrey Baryshev

Groningen Space Research Laboratory and Material Science Center,
P.O. Box 800,
9700 AV Groningen,
The Netherlands.

Sergey Shitov, Andrey Ermakov, Lyudmila Fillipenko, Pavel Dmitriev,

Institute of Radio Engineering and Electronics Russian academy of Science,
Mokhovaya 11,
103907 Moscow,
Russia.

ABSTRACT

A wide band 500 GHz integrated receiver has been designed fabricated and tested. The receiver combines a ring slot antenna SIS mixer with a twin junction type tuning circuit and a Josephson Flux-Flow oscillator as LO. The receiver layout has been made using Nb technology. The receiver chip is glued on the silicon elliptical lens with antireflection coating. According to calculations a 30% 3-dB bandwidth can be achieved with this design. Measured SIS mixer pumping level is sufficient for SIS mixer operation in the band 400-570 GHz. We present the antenna beam pattern of a ring slot antenna on a silicon elliptical lens, a DSB noise temperature of the receiver and a FTS spectrum. The measured receiver DSB noise temperature is analyzed.

Introduction

A single chip heterodyne receiver comprising a Superconductor-Insulator Superconductor (SIS) junction as sensitive element and a long Josephson junction Flux-Flow Oscillator (FFO) as a local oscillator (LO) is very attractive as imaging array in space and airborne applications because of its low weight and power consumption. A double dipole integrated receiver has recently demonstrated a 100 K DSB noise temperature at 500 GHz [1]; which is on the level of state of the art receivers in this frequency band. This receiver had an internal LO (FFO) and had a bandwidth of about 10 %. A possibility to phase lock a FFO to an external reference source in 300-430 GHz frequency band has been shown [2]. This makes it more attractive to design a wide band integrated receiver to utilize a wide tuning range of FFO. The increasing complexity of integrated receivers demands a more accurate analysis of receiver parameters.

In this report a layout of a wide band quasioptical integrated receiver utilizing a one port annular slot antenna is described. The preliminary measurements of receiver DSB noise temperature, receiver beam and integrated control parameters are presented. A receiver DSB noise temperature is analyzed in detail in one frequency

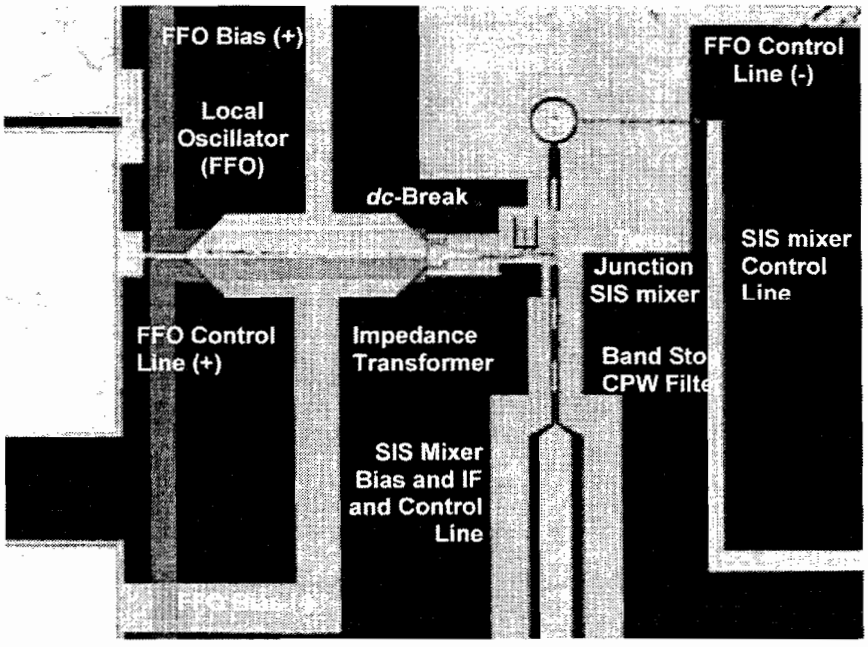

Fig. 1 Photograph of the central part of receiver chip

point.

Receiver layout

The photograph of the central part of the receiver chip is shown in fig. 1.

Quasioptical configuration.

The receiver uses an annular slot line antenna on a silicon substrate. The receiver chip (3 x 4.2x 0.5 mm) is mounted on the flat surface of a (synthesized) elliptical lens such that the center of the antenna is the focal point. An antireflection layer with center frequency 500 GHz covers the front surface of the lens. No additional optical elements are used to form the receiver beam.

Ring slot antenna.

The ring slot antenna is known to have a symmetrical linear polarized antenna beam pattern [3], [4]. It is a compact antenna surrounded by a ground plane. This gives more flexibility to place all strip line elements very close to antenna itself. This antenna doesn't need a blocking capacitor if the central part is made in the wiring layer. The antenna with a circumference of one wavelength for 500 GHz has been chosen. The input impedance of the antenna has been calculated using the momentum method in the Momentum ™ software package as a part of a HP ADS design system. The calculated impedance is shown in fig. 2 and it is in agreement with values used in [3], [4].

LO chain.

A FFO junction has a size of 500 x 4 μm. The three stage tapered strip line impedance transformer is used to convert the low (0.5 Ohm) source impedance to the

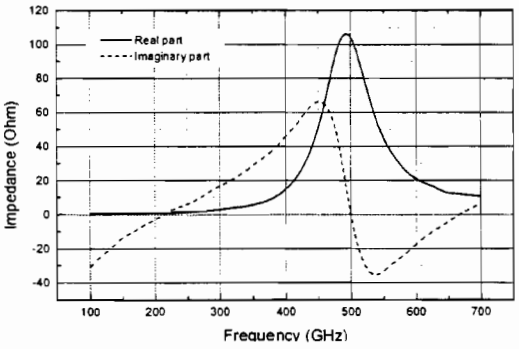

Fig. 2 Impedance of ring slot antenna

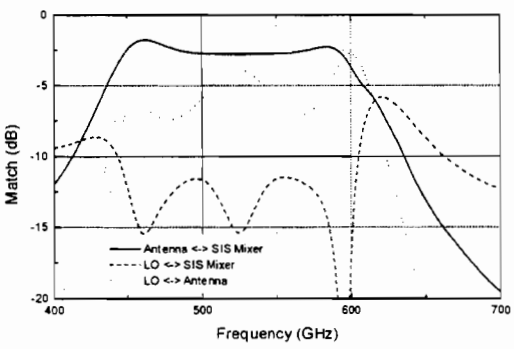

Fig. 3 Calculated layout parameters

level appropriate to combine it with the DC-break. The single insulator layer is used for in first transformer section to decrease its characteristic impedance. The pi-shape DC break is used in order to disconnect the SIS junction bias current and the FFO bias current path. A common ground plane is used throughout the design. The additional micro strip line tuner is used to transform the resulting impedance of LO path to create a required mismatch between LO and detector. This mismatch is needed to avoid leak of a *rf* signal from antenna towards the local oscillator.

The magnetic field for FFO operation is applied by passing current through the bottom electrode along the junction.

Signal chain and SIS tuning elements.

A twin junction tuning circuit [5], [6] is used to compensate the SIS junction geometrical capacitance in wide frequency range. A two stage CPW transformer followed by a one stage strip line transformer is used to match the rather high ring slot line antenna impedance (100 Ohm) to the input impedance of twin junction circuit.

An integrated control line supplies the magnetic field required for suppression of Josephson effect during SIS mixer operation. The control line is placed in the top electrode. Possible leak of *IF* signal should be blocked outside the chip. The return path of SIS junction magnetic field control current is located across the cross-polarized port of the ring slot antenna to avoid the influence to the antenna properties by the other port. A CPW choke filter is used to prevent the leak of *rf* signal towards the bias leads.

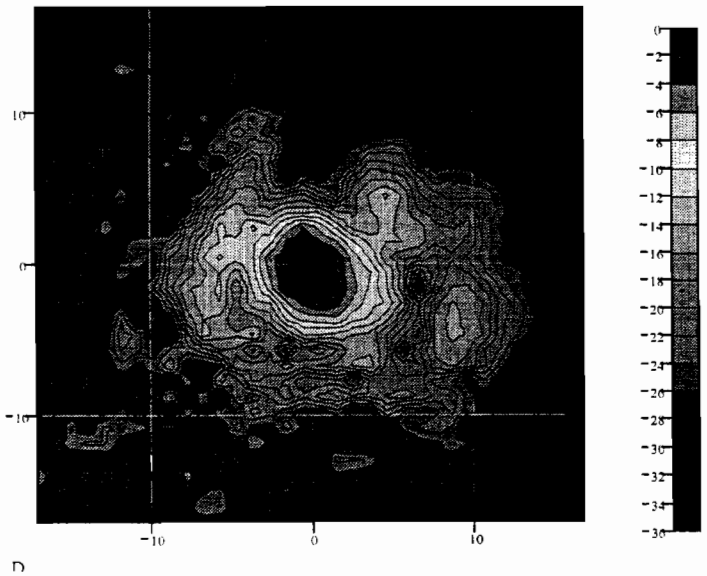

Fig. 4 2D antenna beam pattern of integrated receiver. X-Y axis units: degrees. X-axis corresponds to E-plain. The contour levels are in log scale.

The result of layout calculation for 1.1 x 1.1 μm junction size, 8 kA/cm^2 critical current density and two 135 nm thick insulator layers made of SiO_2 is presented in fig. 3. The mismatch between antenna and twin junction circuit is stable across 30 % bandwidth and is about 1.5 dB. The mismatch between FFO and SIS mixer has been chosen to be 12.5 dB. This level still allows to get sufficient LO power.

Fabrication and Measurement

The first batch of integrated receiver has been fabricated using Nb-AlOx-Nb technology. The SIS junctions size in tuning circuit was estimated to be 1.6 times larger than expected and critical current density was 2 times smaller than required. The only preliminary experimental results can thus be presented.

Antenna Beam Pattern

The antenna beam pattern of antenna lens combination has been measured by scanning a point source in the far field of the lens. A Thomson carcinotron with an horn output blocked by a 1 mm diameter diaphragm has been used as a point source. It allows measuring the antenna parameters within +/- 15 degrees at 500 GHz. The result of the X-Y scan at 475 GHz is presented in fig. 4. It shows the rotationally symmetrical beam with sidelobe level at about –10 dB. The F-ratio of the beam is about #5. Asymmetric excitation of CPW transformer or influence of the edge of ground plane can explain measured sidelobes level.

FFO Test

The pumping level of SIS mixer was measured while scanning the FFO I-V

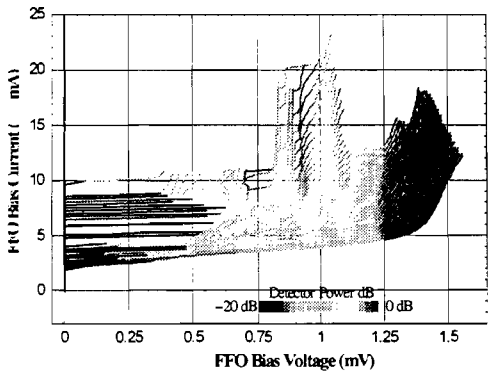

Fig. 5 FFO I-V characteristics. Pumping level is indicated in gray scale. Magnetic field is a parameter.

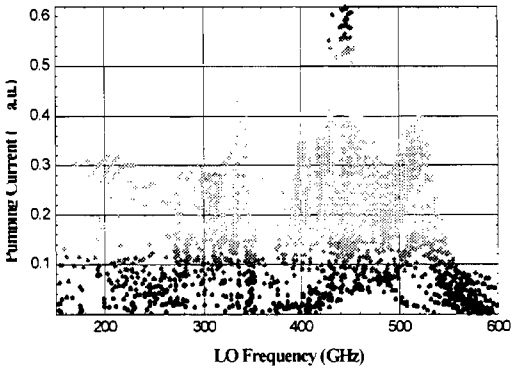

Fig. 6 SIS mixer pumping level vs. FFO frequency.

curve. The recorded set of FFO I-V curves is presented in Fig. 5. Figure 6 shows the measured frequency dependence of the LO level of SIS mixer. The pumping level is sufficient for SIS mixer operation in frequency region 250-550 GHz. It was possible to operate the FFO with magnetic field control line current in the range –30...30 mA and bias current in the range 0...40 mA.

SIS junction magnetic field control line test

The SIS mixer I-V curve has been scanned to determine a critical current while the SIS mixer control line current was changed as a parameter. It was possible to obtain up to third minimum of the critical current without switching the control line in a normal state. The dependence of critical current from the control line current in fig. 7 shows also the SQUID like behavior structure. This is because a twin junction tuning circuit forms SQUID interferometer. The experiment showed that for efficient Josephson effect *IF* noise suppression the first minimum determined by the junction's area rather than the area of SQUID loop is required.

Noise Temperature Measurement

For the noise temperature measurement the receiver has been mounted on the cold plate of LHe cryostat. The input window was made of 10 mkm thick kapton. The 100 mkm thick quartz plate was used as 78 K far infrared radiation filer. The Zitex ™ plate was used as 4.5 K level radiation filter. A circulator and a low noise HEMT amplifier were used in *IF* chain. A directional coupler has been installed between circulator and receiver chip for reflection measurements of SIS junction dynamic resistance at IF frequency. This measurement is required for an accurate estimation of

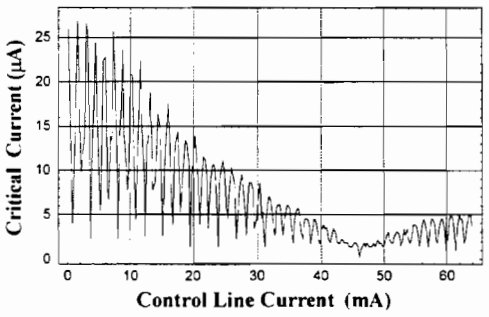

Fig 7 SIS junction critical current vs. magnetic field control line current.

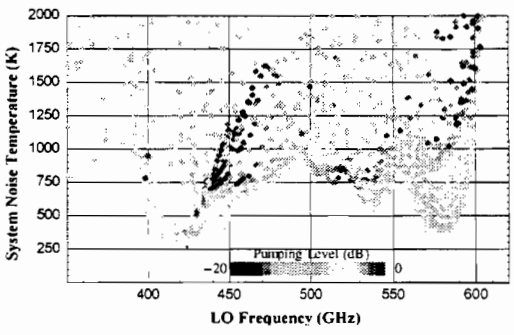

Fig 8 System DSB noise temperature vs. LO frequency. Pumping level is indicated in gray scale.

receiver parameters. The Y-factor has been measured by using two switchable black bodies (78 K/300 K). The IF output power was detected and a calibrated logarithmic amplifier was used to record the Y-factor automatically while scanning the FFO I-V curve. The resulting DSB noise temperature graph is presented in fig. 8. The lowest noise temperature was 300 K for a given production parameters.

Noise Temperature Analysis

The receiver consists of several linear elements connected in series. Each element has its own gain G_i and equivalent input noise power P_i^n. The output power from such an element can be written as $P_{out} = (P_{in} + P_i^n) \cdot G_i$. It is convenient to express all powers in equivalent noise temperatures, because a wide band calibration noise source is used for the measurement. The corresponding noise temperature can be expressed as $P^n = k_b T^n \Delta f$, where Δf is a bandwidth of the intermediate frequency detector. The output power of a linear element can be redefined as $T_{out} = (T_{in} + T_i^n) \cdot G_i$. The receiver gain G_{sys} and the receiver noise temperature T_{sys} can be calculated:

$$G_{sys} = G_1 \cdot G_2 \cdot \ldots \cdot G_k,\ T_{sys} = T_1^n + T_2^n / G_1 + T_3^n / (G_1 \cdot G_2) + \ldots + T_k^n / (G_1 \cdot \ldots \cdot G_{k-1}). \quad (1)$$

The overall receiver performance can be measured using the Y-factor technique. A calibrated black body source can be used to measure G_{sys} and T_{sys}. The properties of all receiver elements can be measured independently except for the *rf* loss in the tuning elements and the lens. This unknown loss of tuning elements and lens can be found by solving (1) when G_{sys} and all other G_k is known. The same is true for the

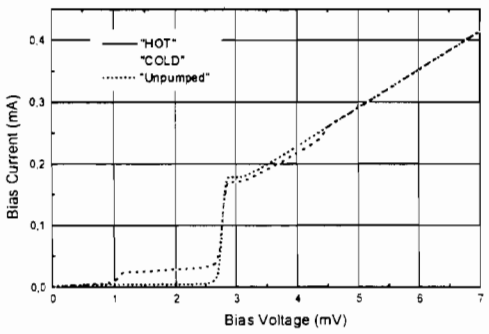

Fig. 9 SIS junction I-V curves.

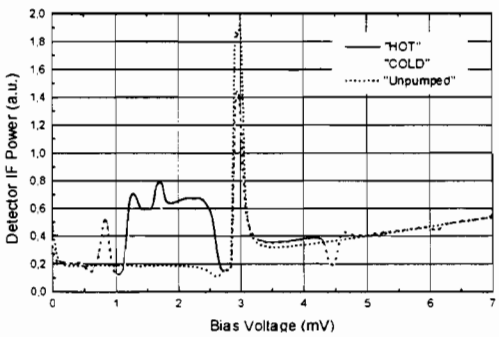

Fig. 10 SIS junction IF output power.

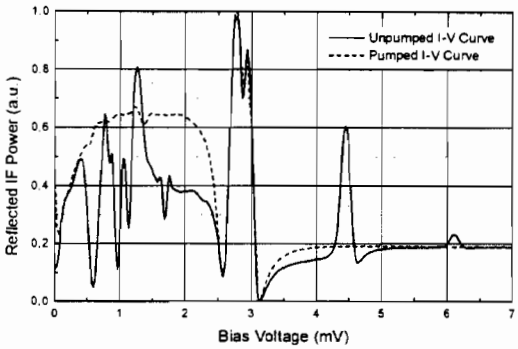

Fig. 11 *IF* port test tone reflected signal for pumped and unpumped I-V curves

noise of this 'element'.

The parameters for the dewar window and all radiation filters can be determined separately by measuring the film transmission with a Micelson FTS spectrometer.

The parameters of the *IF* low noise amplifier chain and detector can be calibrated using the unpumped SIS junction as a calibrated noise source [7]. The noise temperature of the *IF* chain as well as the impedance as seen by the junction at the *IF* port can be determined by fitting the unpumped SIS junction *IF* output power calculated from the measured I-V curve and dynamic resistance to the measured data.

The SIS mixer can be analyzed with the Tucker theory [8]. The information about mixer gain and noise can be obtained from the pumped and unpumped I-V curves and the independently measured dynamic resistance of the junction. Using the measured dynamic resistance allows us to avoid the numerically unstable calculation of the junction's embedding impedance at the *rf* port. A DSB operation of the mixer with equal lower and higher side band parameters is assumed. *Rf* loss due to mismatch in the tuning circuits or non optimal receiver beam efficiency and the associated noise are found using measured receiver parameters. Details of this method will be published elsewhere.

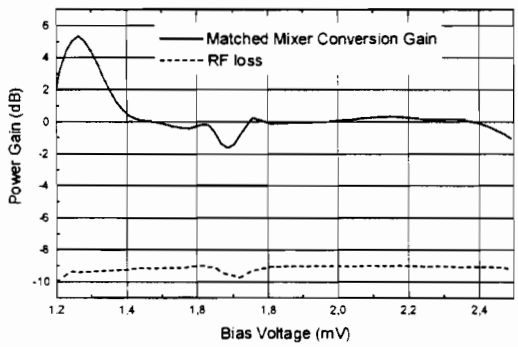

Fig. 12 Calculated *rf* loss and matched mixer conversion gain.

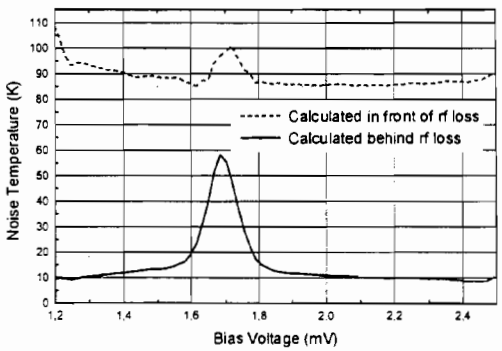

Fig. 13 Noise temperature associated with *rf* loss.

Element	T_I(K)	G (dB)
Dewar Window (10 μm capton)	6	-0.09
IR Filter at 78 K (Quartz Plate)	8	-0.1
IR Filter at 4.3 K (Zitex)	0.3	-0.13
rf Mismatch	73	-9
Mixer Gain Element (Tucker theory)	86	0.16
if Mismatch	38	-1.9
if Amplifier and Detector	91	0
Receiver	302.3	-10.93

Table 1. Receiver elements noise temperature (recalculated to the front of receiver) and gain for bias point of 2 mV and *LO* frequency 410 GHz.

Noise Temperature Analysis Result and Discussion.

Experimental data needed for the receiver analysis is shown in fig. 9-11. The analysis is made for a *LO* frequency of 410 GHz. Based on these curves one can calculate the noise budget for all receiver components. The matched mixer conversion gain along with the calculated *rf* loss is shown in fig. 12. The value of the *rf* loss should not depend on the bias voltage across the first photon step. This is seen from the measurement despite the varying mixer gain. The noise temperature associated with *rf* loss is shown in fig. 13. It corresponds to a level of approximately 85 K referred to the front of the receiver and 10 K if it is attributed after this element. The value of 10 K is the zero-point fluctuations level at this frequency. The ripple near bias voltage of 1.7 mV corresponds to the position of second Shapiro step and reflects the additional noise due to Josephson effect. A noise temperature and gain budget for the receiver is shown in table 1. Noise temperature is referred to the input of the receiver, so the receiver noise temperature can be obtained by adding all contributions. From the table follows that the main contribution to the system noise temperature arises from *rf* loss. This loss is due to increased junction area.

Acknowledgements

Authors would like to thank Teun Klapwijk, Willem Luinge, Herman van de Stadt and Valery Koshelets for stimulating discussions. The work was supported in parts by the Russian Program for Basic Research, the Russian SSP "Superconductivity", ESA TRP contract 11653/95/NL/PB.

Conclusion

A wide band integrated receiver layout with a ring slot line antenna and a twin junction tuning circuit has been developed. Calculation showed 30% instantaneous bandwidth. The preliminary experiments showed that this design could be used as a wide band integrated receiver for frequencies of 400...550 GHz. The receiver noise temperature analysis demonstrated stable receiver parameters across first photon step of SIS junction and shows the most critical parts of the measurement setup.

References

[1] S.V. Shitov, A. B. Ermakov, L. V. Filippenko, V. P. Koshelets, A.M. Baryshev, W. Luinge, Jian-Rong Gao, *Superconducting Chip Receiver for Imaging Applications*,. Was presented at ASC-98, Palm Desert, CA, USA, Report EMA-09, (1998), to be published in IEEE Trans. on Appl. Supercond. (1999).
V.P. Koshelets, S.V. Shitov, L.V. Filippenko, A.M. Baryshev, H. Golstein, T. de Graauw, W. Luinge, H. Schaeffer, H. van de Stadt, *First Implementation of a Superconducting Integrated Receiver at 450 GHz*, Appl. Phys. Lett., Vol. 68, No. 9, pp. 1273-1275, 1996.

[2] V. P. Koshelets, S. V. Shitov, A. V. Shchukin, L. V. Filippenko, P. N. Dmitriev, V. L. Vaks, J. Mygind, A. M. Baryshev, W. Luinge, H. Golstein, *Flux Flow Oscillators for Sub-mm Wave Integrated Receivers.* Was presented at ASC-98, Palm Desert, CA, USA, Report EQB-04, (1998), to be published in IEEE Trans. on Appl. Supercond. 1999.

[3] C.E. Tong, R. Blundell, *An Annular Slot Antenna on a Dielectric Half-Space*, IEEE Trans. On Ant. and Propagation, vol. 42, No 7, pp. 967-974, July 1994

[4] S. Raman, G.M. Rebeiz, Single – and Dual-polarized Millimeter-Wave Slot-Ring Antennas, IEEE Trans. On antennas and propagation, vol 44, no. 11, pp. 1438-1444, Nov 1996

[5] Belitsky V.Yu., Jacobsson S.W., Filippenko L.V., Kovtonjuk S.A., Koshelets V.P., Kollberg E.L., *0.5 THz SIS Receiver with Twin Junctions Tuning Circuit.*, Proc. 4th Space Terahertz Technology Conference, p.538, March 30 - April 1, Los Angeles, USA.,1993

Belitsky V. Yu., Tarasov M.A., "SIS Junction Reactance Complete Compensation", IEEE Trans. on Magnetic, MAG- 27, v. 2, pt. 4, pp. 2638-2641., 1991

[6] M.C. Gaidis, H.G. Leduc, Mei Bin, D. Miller, J.A. Stern, and J. Zmuidzinas, *Characterization of Low Noise Quasi-Optical SIS Mixers for the Submillimeter Band*, IEEE Transactions of Microwave Theory and Techniques, p. 1130-1139, 1996

[7] Belitsky V.Yu, Serpuchenko I.L., Tarasov M.A., *Shot Noise In Superconducting Single Junction And Arrays*, 5th Conf. on WEAK

SUPERCONDUCTIVITY, Smolenice, Czechoslovakia. May 29 - 2 June 1989, Nova Science Publisher, ISBN 0-941743-78-0 Conf. Proc. pp. 191-195, 1990

D.P. Woody, *Measurement of the Noise Contributions to SIS Heterodyne Receivers*, ASC'94 Proceedings, 1995

[8] R. Tucker, M.J. Feldman, *Quantum Detection at millimeter wavelengths*, P.1055-1112, Reviews of Modern Physics, Vol. 57, No. 4, October 1985

A.R. Kerr, M.J. Feldman, S.-K. Pan *Receiver Noise Temperature, the Quantum Noise Limit, and the Role of the Zero-Point Fluctuations*, Eight Int. Symp. on Space Terahertz Technology proceedings, p. 101-111, 1997.